

N90-22081

DEVELOPMENT OF SHAPE MEMORY METAL AS THE
ACTUATOR OF A FAIL SAFE MECHANISM

V. G. Ford*, M. R. Johnson*, and S. D. Orlosky**

ABSTRACT

A small, compact, lightweight device has been developed using shape memory alloy (SMA) in wire form to actuate a pin-puller that decouples the flanges of two shafts. When the SMA is heated it contracts producing a useful force and stroke. As it cools, it can be reset (elongated in this case) by applying a relatively small force. Resistive heating is accomplished by running a current through the SMA wire for a controlled length of time. The electronics to drive the device are not elaborate or complicated - consisting of a timed current source. The total available contraction is 3% of the length of the wire. This paper describes this device, the engineering properties of the SMA, and the tests performed to verify the design concept.

INTRODUCTION

The Wide Field Planetary Camera (WFPC) on the Hubble Space Telescope detects electromagnetic radiation in a broad wavelength range from infrared to ultraviolet. There are two WFPC units - the first (WFPC I) is expected to be launched in March 1990, and the second (WFPC II) is a replacement unit expected to replace WFPC I on a follow-up mission. During the qualification test cycle for WFPC I, it was observed that contaminant deposition on the lens surfaces and on the detector blocked short wavelength radiation, preventing the desired transmission and reception of ultraviolet light. Additionally, a window that seals the aperture of the optical path of WFPC I from the outside environment also reduced the transmission of ultraviolet radiation by more than 80%.

Several refinements have been adopted for WFPC II to improve the transmission of ultraviolet. More stringent controls on materials used in the instrument have been maintained. Additionally, a new detector with more sensitivity in the ultraviolet was developed. Finally, the aperture window was mechanized for WFPC II to swing out of the optical path after the satellite and its payload have been exposed to space long enough to have outgassed sufficiently.

* Jet Propulsion Laboratory, California Institute of Technology, 4800 Oak Grove Drive, Pasadena, California 91109

**TiNi Alloy Company, 1144 65th Street, Unit A, Oakland, California 94608

The Aperture Window Mechanism had to fit within a small available volume and to use existing electronics with as little modification as possible. If a failure occurs in the motor or electronics of the window drive, the mechanism was required to have an override system that moves the window to the open position. The override is known as a fail-safe function.

The SMA device that will be described in this paper is the component of the Aperture Window Mechanism that actuates the fail-safe function. If the motor or drive train of the window fails, this component releases a preloaded torsion spring that will drive the window to the open position. A design goal of this component was to have low mass and volume, to require little modification to existing electronic controls, and to be as simple as possible.

Figure 1 shows the Aperture Window Mechanism assembled in the mechanisms housing of WFPC II. A four-bar linkage has an over-center position that spring-loads and latches the frame of the window against a machined surface of the housing in the closed position. Figure 2 shows a cross-section of the mechanism actuator. A motor drives the wave generator of a harmonic drive that turns an output shaft. The coupling flange on the shaft houses the SMA fail-safe actuator to be described in this paper. The coupling flange also

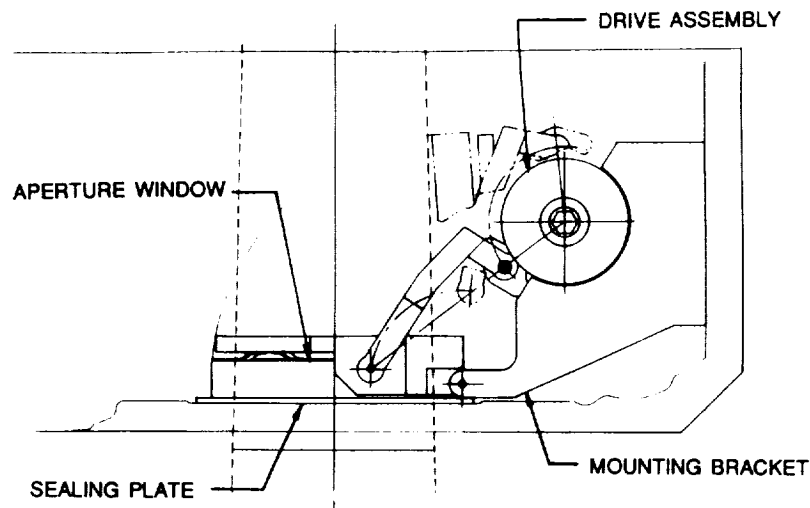


Figure 1. The Aperture Window Mechanism of WFPC II

has a feature that engages one end of the torsion spring. During normal operation, the torque from the drive shaft is transmitted through the coupling flange to the fail-safe actuator, through its plunger to the drive link of the four-bar. The drive link is flanged to retain the plunger in a slot and has a

feature to preload the other end of the torsion spring. When fail-safe action is required, the plunger is pulled, the torsion spring preload is released, and the drive link is forced to the open position.

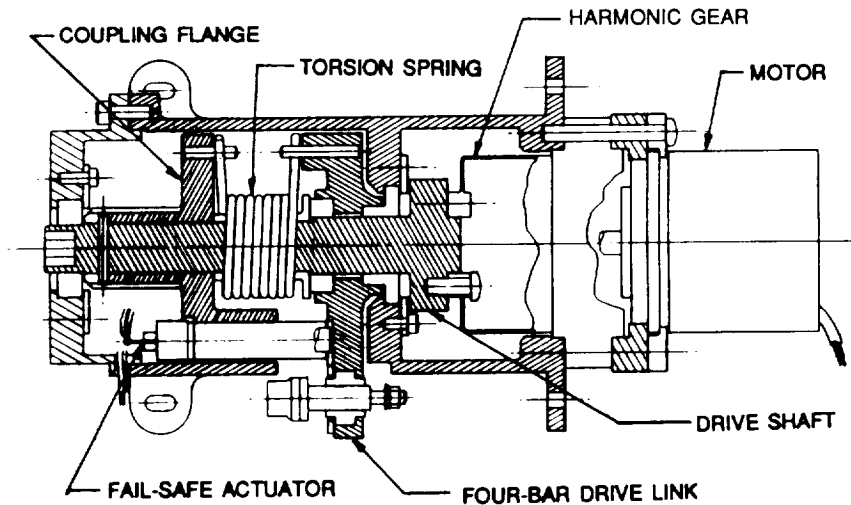


Figure 2. Cross-Section of the Aperture Window Mechanism Actuator

FAIL-SAFE ACTUATOR DESIGN

The fail-safe actuator is a pin puller device as shown in Figure 3. It consists of a preloaded plunger that engages a slot. A compression spring presses against a spring retainer that pushes the plunger causing it to be forced into the slot. Redundant SMA wires loop around the end of an insulated core which engages the plunger. When current passes through the wires they are heated and contract, pulling the core against the spring load and the friction load of the sliding plunger.

Figure 4 shows an exploded isometric of the actuator with its parts labeled. The interface to the Aperture Window Mechanism is the plunger, which is made of Nitronic 60 CRES. This material was chosen for its hardness of approximately R_c43 and gall resistance. The applied force is 31 pounds in shear across the face of the plunger. The hard material, combined with a fine surface finish, provides a low coefficient of friction when sliding is required against the coupling flange of the Aperture Window Mechanism. This flange is hard anodized aluminum with a surface infusion of molybdenum disulfide. The low coefficient of friction minimizes the required output

force from the actuator.

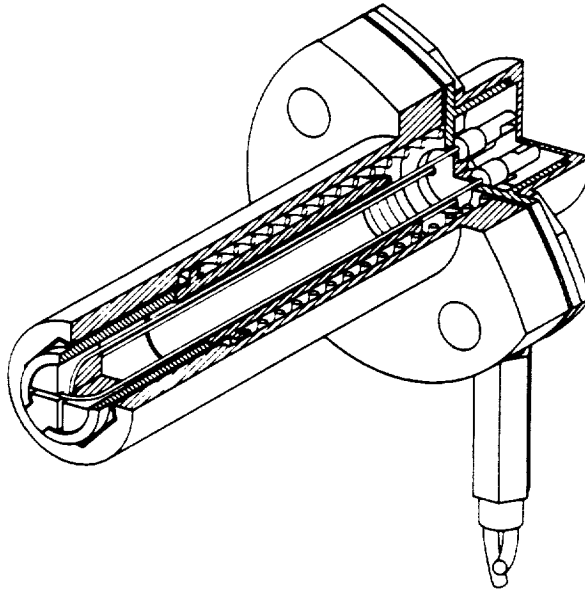


Figure 3. Cut-Away Isometric of the Fail-Safe Actuator

Since the SMA wires actuate by resistance heating, they must be insulated from each other and the rest of the mechanism. The core performs this function. It is constructed of a polyimide resin, Vespel SP-1, to provide the necessary insulation, heat transfer resistance, and force transmission from the wires to the plunger. The details of the cruciform shape in the end of the core guides and insulates the two SMA wires, allowing them to cross perpendicularly without contacting each other.

The spring in the actuator performs a dual function. It preloads the moving mass of the plunger assembly in the extended position. This provides resistance to unlatching during the expected vibration and shock environment and raises the natural frequency of the moving components. The spring also provides the force necessary to extend the SMA wires during their transition to the martensitic state by exceeding the chosen martensitic plateau stress of 5000 psi. This will be discussed further in the next section.

The spring insulator is made of Vespel SP-1 and prevents electrical contact between the SMA wire and the BeCu spring. It forms the mandrel for the spring locating it between the spring insulator and the bore of the device housing. The spring insulator also limits the stroke of the plunger assembly, preventing excessive strain in the wire.

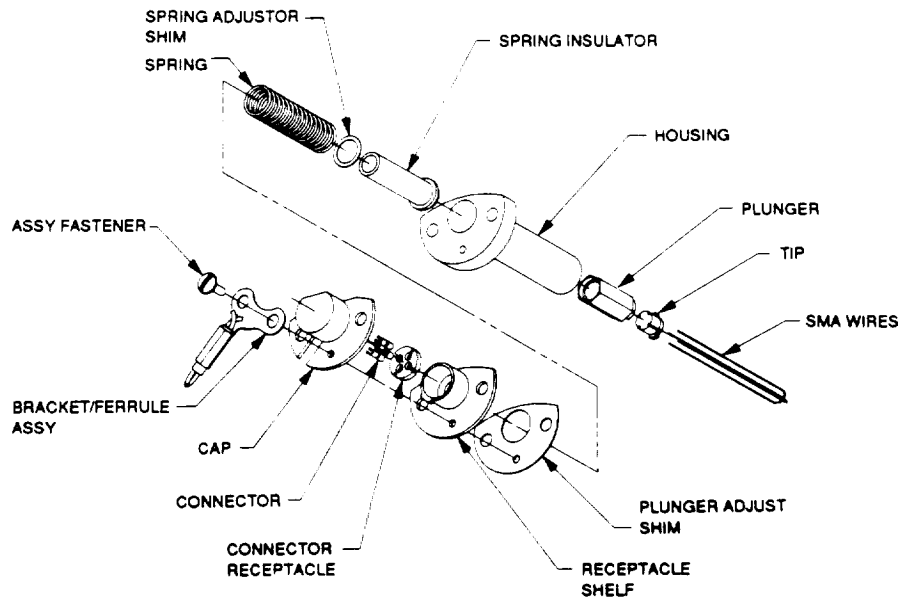


Figure 4. Exploded-View Isometric of the Fail-Safe Actuator

The housing is made of titanium 6Al-4V. This material was chosen for its ability to carry the bending stresses induced by the loading of the fail-safe actuator. A portion of the bore is hexagonal to prevent any rotation of the plunger that would twist the SMA wires. The hexagonal portion is anodized with a surface infusion of molybdenum disulfide that lowers the coefficient of friction and forms a non-galling surface in contact with the plunger.

Electrical contact and mechanical retention of the SMA wire is accomplished with special connectors. The connectors mechanically prevent the wire from slipping, thus are essential for maintaining the tension in the wires. The connectors are purchased from Raychem Corporation of Menlo Park and are shown in Figure 5. They consist of a beryllium copper socket that is slit like a tuning fork, forming tangs that are then bent outward. A ring made of a proprietary SMA alloy called Tinel is used to squeeze the tangs to grip a wire that passes through the socket. The Tinel ring is slipped over the outside diameter of the socket, forcing the tangs to return elastically to their unbent position. When the connector is cooled to -90 C (below the transition temperature of Tinel) the ring material transforms to low strength martensite. The stored spring energy of the tangs deforms the ring into a larger oval shape. The SMA wire is inserted through the connector at this lowered temperature. As the connector warms toward ambient temperature, the ring goes through transition to Austenite and returns to its original smaller round shape, pulling in the tangs and clamping the wire tightly. The

retention capability is high, typically above 22 Newtons (5 lb). For assembly, the connector is dipped into liquid nitrogen, the wire is slipped through the connector, then as the connector warms up, the wire is squeezed into place. The connector body is radiused to eliminate possible stress concentrations in the SMA wire that might reduce the life of the actuator. The high compressive force on the wire creates a gas-tight joint resulting in a low electrical resistance and a high corrosion resistance.

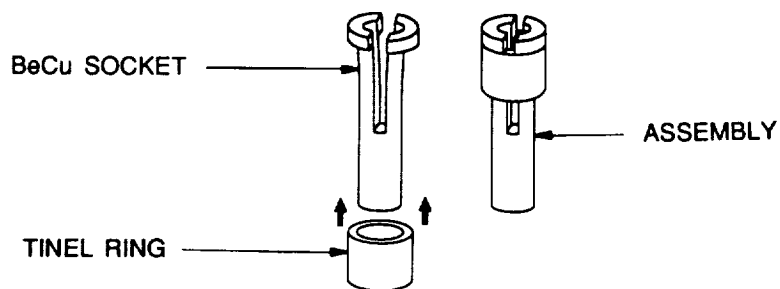


Figure 5. Connector Made of Beryllium Copper and Tinel

The actuator is assembled by first installing the connectors on the SMA wires, then sliding the looped wires through the plunger and the housing. The plunger core is inserted by looping the SMA wires around its two grooves. The spring insulator, the spring adjustor shim, and the spring are next inserted in order into the housing. The plunger shim and the receptacle shelf are placed on the housing flange. The spring is compressed and the connectors are slipped through slots onto their receptacle, which is guided into the receptacle shelf to form the preloaded assembly.

Pigtails are then soldered onto the connectors, after which the cap is installed with the assembly fastener. The wires slip over the lip on the receptacle shelf through a slot on the cap to be clamped in the bracket/ferrule assembly that is also attached to the housing with the assembly fastener. When the actuator is mounted to the coupling flange of the Aperture Window Mechanism, the mounting hardware redundantly retains the bracket/ferrule assembly and the cap against the flange. Figure 6 shows orthographic projections of the actuator with overall dimensions labeled.

Due to contamination concerns, all polymers in the fail-safe actuator were limited to be Vespel SP-1. This material meets the stringent outgassing requirements of WFPC II and has good engineering properties.

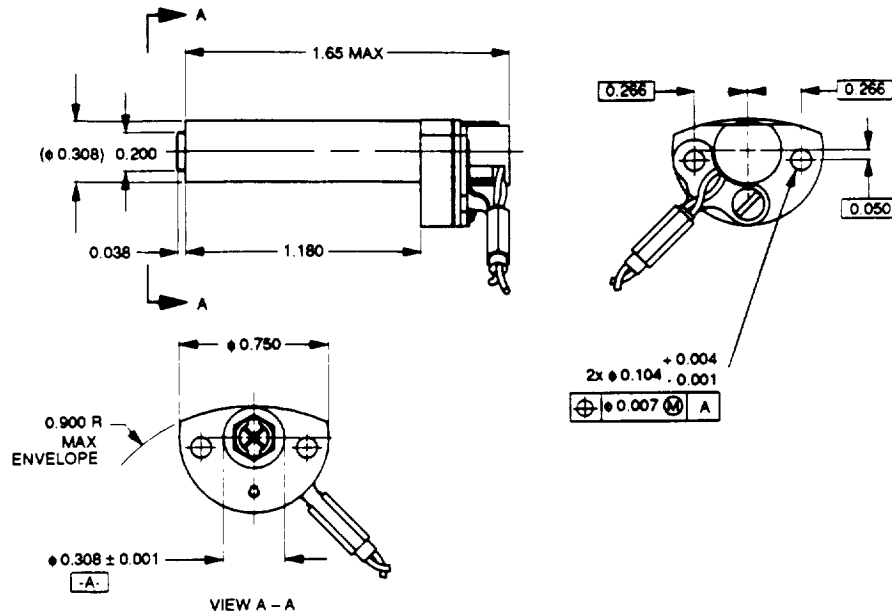


Figure 6. Orthographic Views of the Fail-Safe Actuator

PROPERTIES OF TITANIUM-NICKEL SHAPE-MEMORY ALLOY

Shape-memory alloy designates a class of materials which exhibit a pronounced change in stress-strain characteristics over a narrow temperature range. The most common of these, an alloy of nickel and titanium commonly referred to as Nitinol, was the material chosen for use in the fail-safe actuator.

The advantages of nickel-titanium shape memory alloy for this application are its large work output per unit volume (a typical value is 10 joules/cm³ [1]), electrical resistivity which makes it suitable for direct Joule heating, a long fatigue lifetime, and a non-reactive chemistry. The disadvantages of TiNi are: thermal energy conversion efficiency is low (of the order of one or two percent), and the cycle rate is slow because of the need to dissipate heat. These are not serious disadvantages in the present application.

Good design practice in using shape-memory alloy wire includes careful handling and retention to prevent creation of surface defects which can propagate as cracks, limiting current so that the actuator is not overheated, and limiting strain to about three percent. Failure to observe these limitations can lead to unstable behavior in which the wire changes length from one cycle to the next, and to premature failure. A correctly installed and operated SMA wire actuator can be expected to operate for millions of

cycles with a high degree of repeatability.

There is no convenient method of soldering wires made of nickel-titanium. Swaged or crimped electrical connections which have sufficient mechanical strength to function as mechanical attachments, and which have long useful lifetimes, have been developed. For the purposes of this design, the beryllium copper-Tinel connector was chosen to enable easier inspection of the contact area.

Power requirements for driving an SMA wire are a function of the wire diameter chosen to produce the necessary forces, the length of material needed to perform the required movement, and the speed with which the actuation takes place. The physical size of the SMA actuator is chosen to meet mechanical requirements of the system. A relationship exists between the speed of actuation for an SMA element and the current density (amps/mm²) through the material. Based on this relationship and the current available to perform the actuation, the speed of performance is determined.

Use of shape-memory materials for actuation requires an understanding of how the stress-strain properties of the metal change with temperature and how this change can be used to extract work. For most practical applications an SMA actuator can be treated as a two state device: in its low-temperature state, it is pliable and easily deformed while in its high-temperature state it is rigid and very strong. Referring to Figure 7, these two states have been illustrated on a stress-strain diagram. The high-temperature (austenite) state shows a rather conventional elastic curve. The low temperature (martensite) state, however, exhibits a pronounced plateau of plastic

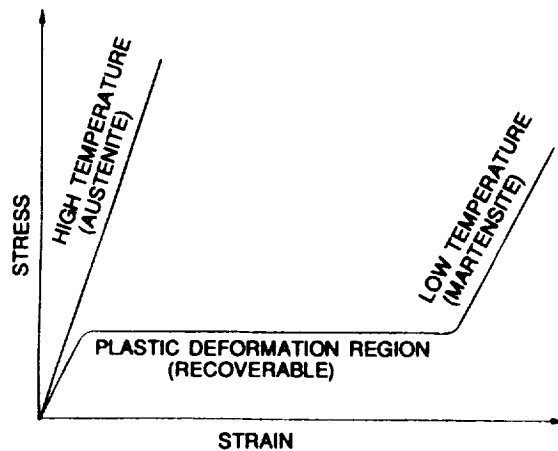


Figure 7. Stress-Strain Diagram of Austenitic and Martensitic States of Nitinol

deformation at a specific stress level. This plastic deformation is recovered (the material "remembers" its high temperature state) when heated above its transition temperature. A plot of length versus temperature illustrates this in Figure 8, in which a typical hysteresis loop appears. Depending on the processing of the material the plateau can occur anywhere in the range of from 0 to about 104 MPa (15,000 psi) [2]. Furthermore the maximum stress in the material was limited to 208 MPa (30,000 psi). This latter limit, based on operational experience [3], produces designs which are reliable over many cycles of operation. Much higher recovery stresses are possible, but cycle lifetime is thereby reduced.

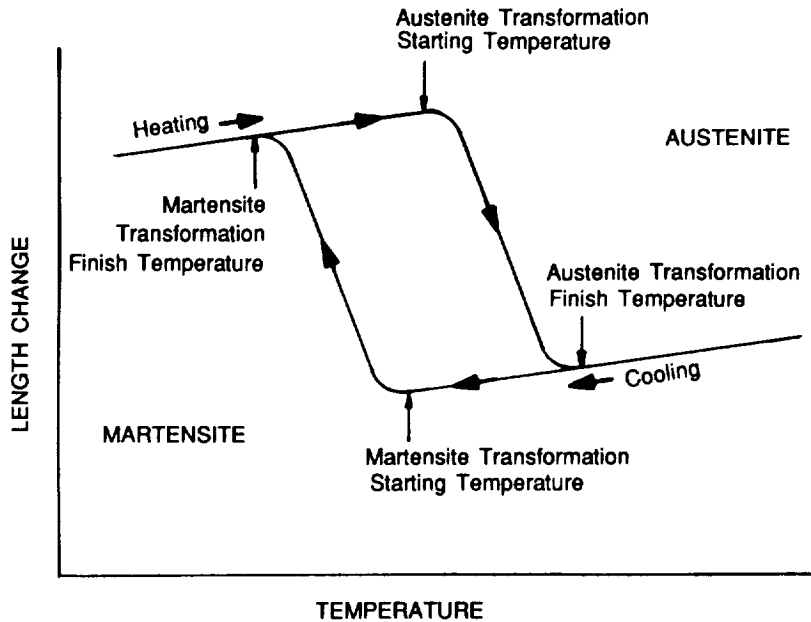


Figure 8. Length Change Versus Temperature of SMA Wire Under Constant Stress

Actuators take advantage of these changes in properties to produce useful work. In operation of the actuator, loading on the SMA wire comes from two sources: the return spring exerts a linearly increasing force during actuation, and a friction load is exerted when the pin moves. For test purposes, the friction load is assumed constant over the entire stroke length of the actuator. These two loads are shown in Figure 9. The entire actuation cycle is illustrated in this figure. As the cold wire is heated, the stress rises from point A to B before movement begins. When the friction load is overcome, the wire starts to pull the plunger, compressing the spring and increasing the stress to point C as the SMA completes the transition to austenite. When power is discontinued, the wire cools and reverts to the ductile low-temperature phase. The spring then overcomes the force of the SMA, and it elongates as the plunger returns to its original position.

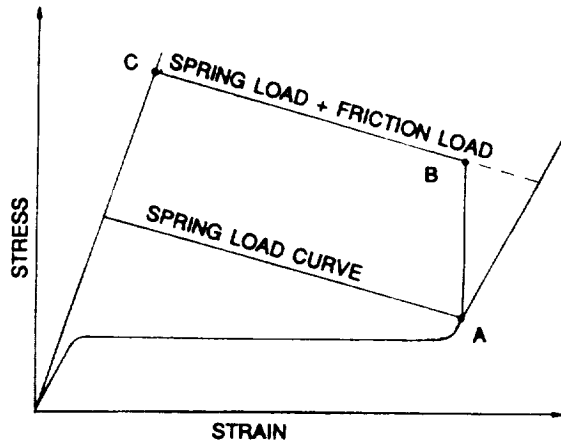


Figure 9. The Force Recovery Cycle of the Nitinol Wire Actuator

ACTUATOR PERFORMANCE TESTING

A simplified version of the flight component was developed by TiNi Alloy Company to test and demonstrate the concept of the SMA actuator. Figure 10 shows this breadboard set-up. SMA (Nitinol) wire 0.203 mm (0.008 in.) in diameter was looped around a grooved Vespel pin. The groove in the pin retained, guided and insulated the SMA wire. The Vespel pin slid through an aluminum flange mounted to a steel shaft. The pin was loaded with a compression spring to tension the SMA and to reach into a slot machined in an adjacent retaining flange. In the back of the pin, a rod was pressed axially into a small hole, then extended to carry the core of a Linear Variable Differential Transducer (LVDT) that measured displacement of the pin. The retaining flange was mounted on bearings that rotated around the steel shaft. A cable wound around the retaining flange at a radius of one inch. Torque loads were applied to the system by hanging weights from the cable to duplicate the torque load of the torsion spring of the Aperture Window Mechanism. The weights were removed and changed to alter the test load. The pin was placed at a radius of 19 mm (0.75 in.), thus the SMA wire had to pull against the friction generated by forces on the pin against the slots in the aluminum flanges. Thin aluminum tubes were crimped to the ends of the SMA wire to mechanically retain the wire and to provide an electrical contact surface where current-carrying wires were soldered. In this case, the crimping was considered for breadboard purposes only - not for aerospace applications.

As the device was actuated, force, current, displacement, resistance and temperature were monitored. The device was powered by a square wave current pulse generator controlled to deliver one pulse. The duration and amplitude

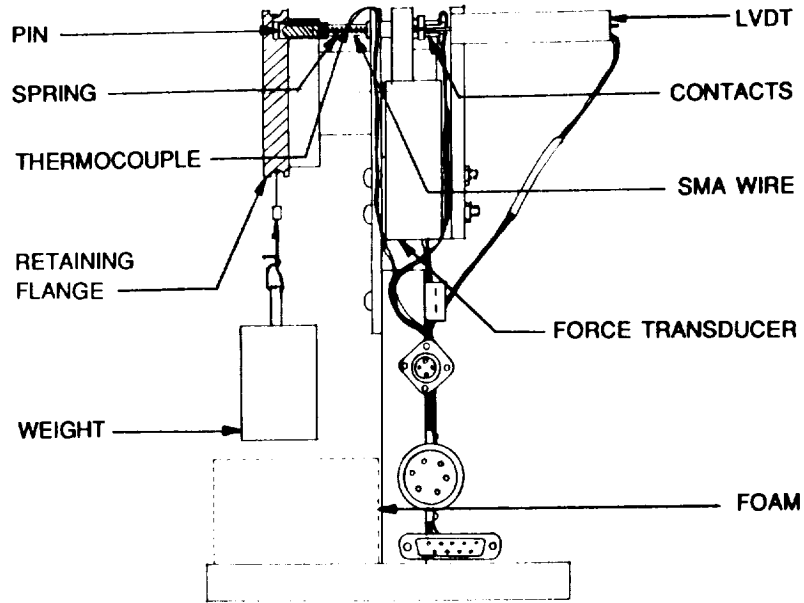


Figure 10. Breadboard Set-Up to Test the SMA Actuator Concept

were variable, with the current to the SMA monitored by measuring the voltage across a 1 ohm resistor and the pulse length read off the screen of a memory oscilloscope. A force transducer measured the force on the pin. Displacement was monitored using the calibrated LVDT voltage output. Resistance was measured by monitoring the voltage across the SMA wire. A thermocouple was epoxied onto the surface of the SMA wire to measure its temperature. Force versus stroke testing was done at TiNi Alloy Company, using a PC-based testing system that monitored the LVDT and force transducer outputs. At JPL, a memory oscilloscope was used to plot resistance, current, displacement and temperature versus time.

TEST RESULTS

Figure 11 shows a plot of TiNi Alloy Company test results comparing force delivered by the SMA wire versus distance moved by the pin. In this plot, a peak force of 12.1 Newtons (2.7 pounds) was reached, and the pin moved a total distance of .72 millimeters (.028 inches). The torque load applied to the flange was 497 Newton-mm (4.4 in-lbs) and the current was constant at 1.2 amps during this actuation. This peak force is equivalent to a peak stress of 187 MPa (26,900 psi) which is 90% of the stress limit of 208 MPa (30,000 psi) that was adopted to prevent elongation during cycling. During testing at JPL, the torque load on the flange was varied from zero to 565 N-mm (5.0 in-lb).

Current was also varied to demonstrate the device sensitivity to current stability.

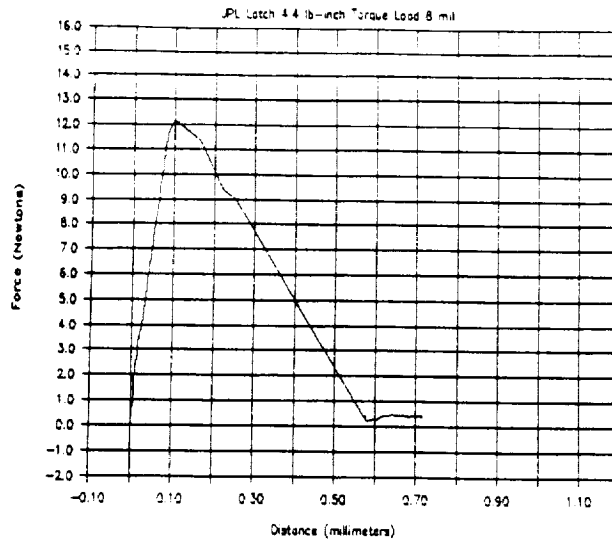


Figure 11. Force Versus Distance Plot of 0.008 Inch Nitinol Wire

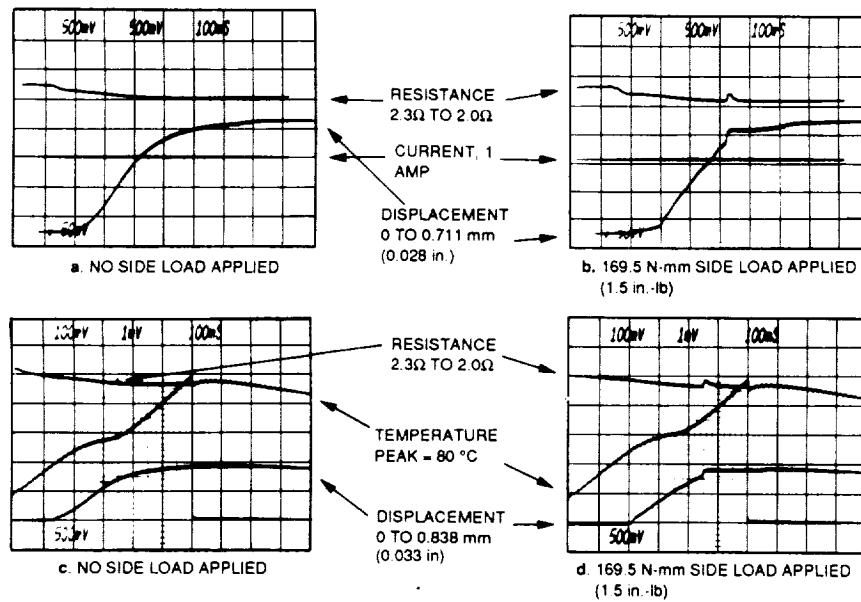
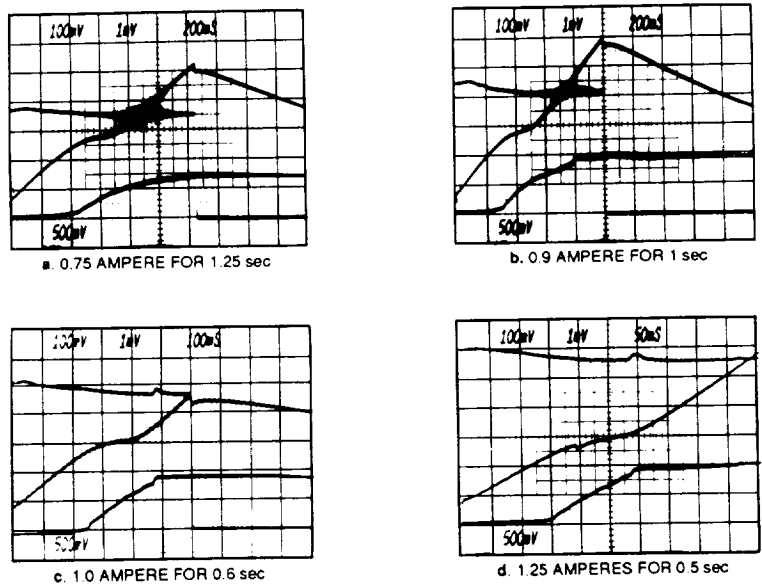


Figure 12. Oscilloscope plots showing device actuation under no-load and load conditions using one ampere current pulse through 0.203 mm (0.008 in.) diameter SMA wire.

Figure 12 shows oscilloscope plots where resistance, current, displacement and temperature were monitored. In Figure 12a, no torque load was applied, the resistance of the SMA wire went from 2.3 to 2.0 ohms as it heated, the current applied was 1 amp for a duration of 900 milliseconds, and the displacement of the pin was 0.86 millimeters (0.034 inches). Figure 12b shows a plot of the same conditions, except that a 1.5 inch-pound load is applied. The total displacement of the pin is identical to the unloaded condition, though the side load created a more pronounced step when the pin began moving and when it broke loose from the retaining slot. Figures 12c and d are plots of the identical conditions as 12a and b respectively, except that displacement, resistance and temperature were monitored.

In Figure 13, the displacement, resistance and temperature were monitored with an applied torque load of 1.5 in-lb with varying current conditions. The table at the bottom of the figure summarizes the four



| | Current (amp) | Pulse Length (sec) | Peak Temp (C) | Movement Threshold Temp. (C) | Actuation Temp. (C) | Maximum Displacement (mm) | Actuation Time (sec) |
|---|---------------|--------------------|---------------|------------------------------|---------------------|---------------------------|----------------------|
| a | 0.75 | 1.25 | 80 | 47 | N/A | 0.55 | N/A |
| b | 0.9 | 1.0 | 112 | 48 | 91 | 0.91 | 0.80 |
| c | 1.0 | 0.9 | 122 | 48 | 72 | 0.89 | 0.54 |
| d | 1.2 | 0.5 | 122 | 49 | 65 | 0.89 | 0.28 |

Figure 13. Oscilloscope plots showing performance against a side load of 169.5 N-mm (1.5 in-lb) with varying currents.

conditions and the resulting data. At the lowest current shown, 0.75 Amps, actuation did not occur though the transition had begun. The difference in actuation temperatures is due to the time lag of heat transferred through the epoxy to the thermocouple. The peak temperatures achieved are a function of current level, pulse length, and heat transfer from the SMA wire.

In Figure 14, the torque load was increased to 5 inch-pounds and the current was 1.2 amperes with a pulse length of 0.5 seconds. This configuration was cycled over 200 times until failure. The failure occurred at one of the crimp contacts which started slipping, emphasizing the need for more careful anchoring.

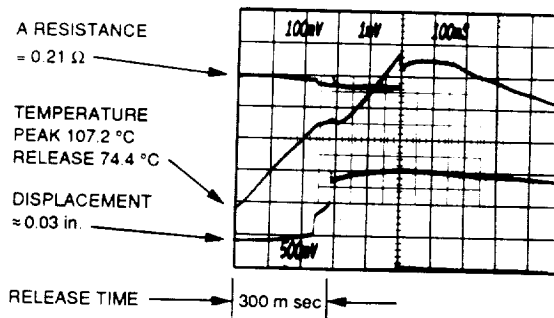


Figure 14. Plot of actuation with a side-load of 565 N-mm (5 in-lb) with an applied current of 1.2 amps for 0.5 seconds.

At the time of writing this paper, no further testing has been done. Full qualification testing is expected on an engineering model and on protoflight units to be built. Some of this testing is expected to be finished by the time the paper is to be presented, and will be included in the presentation.

CONCLUSIONS

The goal of the testing done was to establish the flexibility of this device to the varying environments it could potentially encounter. Testing in thermal-vacuum conditions was not funded at the time, so the tests performed concentrated on current variations and time variations in the laboratory environment. The testing was to establish minimum limits of current and time that would actuate the device, and to test the maximum limits to ensure that the device would not overheat within the expected times for actuation. Because life cycling and demonstration of the device was planned, the testing did not try to establish maximum conditions that would cause failure of the SMA wire. The minimum limits established were that actuation would occur

reliably with a current of 0.9 amps for a duration of greater than 0.8 seconds. The actuator performed well with a current of 1.2 amps for 0.5 seconds, reaching a peak temperature measured at 109 C. At the current level of 1.2 amps for 0.5 seconds, no degradation was observed during cycling. Figure 15 shows a plot of the data points collected at JPL superimposed on the

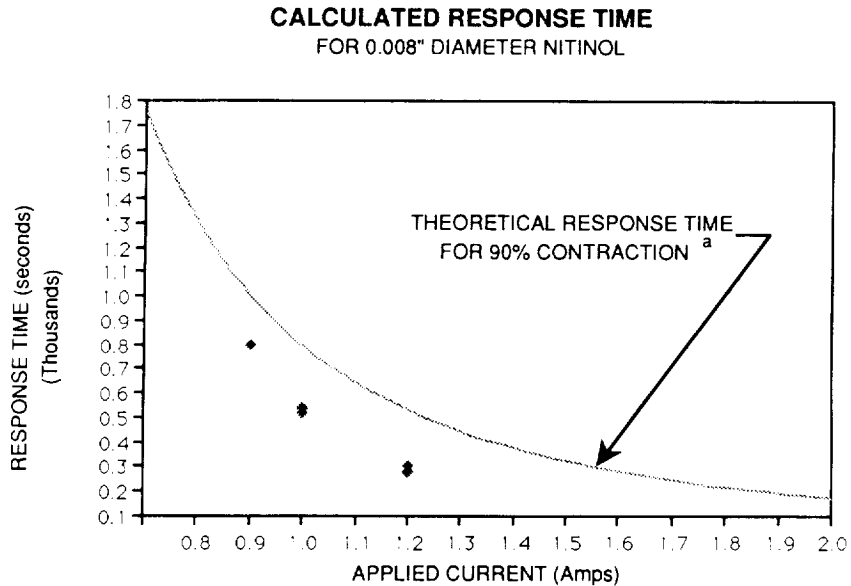


Figure 15. Response time versus current for 0.203 mm (0.008 in.) diameter Nitinol in still air.

calculated theoretical response curve for 90% contraction of the SMA wire. The curve represents the response time versus applied current of Nitinol wire in still air at 20 C. The breadboard device appears to be actuating at less than 90% contraction, and to follow the theoretical curve very closely.

To characterize this device adequately for aerospace applications, thermal-vacuum testing must be done. All the testing described above was done in a laboratory environment with an ambient temperature of 21 C. The heat transfer conditions in a vacuum will greatly affect current level and duration required for actuation. It is expected that actuation will occur at lower current levels, with shorter response times. The wire may overheat more readily. The testing that is planned will help establish response curves for the wire in a vacuum. The wire currently planned for the engineering model will have a larger diameter which will affect the current, response time and temperature relationship. This also will be characterized by further testing.

a. Based on empirical studies performed at TiNi Alloy Company.

STATUS OF THE ACTUATOR

Several design changes were required after the breadboard testing phase was completed. The required preload on the aperture window was raised which increased the friction load on the plunger. Because of this, the diameter of the SMA wire was increased to provide more force when actuated. Hardware development of the flight version of the fail-safe actuator is currently through the detail drawing stage. The fail-safe actuator is scheduled for design review in January 1990. Development and component testing are scheduled to take place from January through May of 1990. The procurement of the SMA connectors to be used in the design is already in process. The flight testing of the Aperture Window Mechanism is scheduled for November 1990 with assembly in the WFPC II to begin in January of 1991. The assembled WFPC II is scheduled to be sent to Goddard in August of 1992 for preparation for launch on the replacement mission.

REFERENCES

- [1] A. D. Johnson, A. D. "Experimental Results on a Continuous Band Nitinol Engine," Proceedings of the Nitinol Heat Engine Conference, NSWC MP 79-441, Sept. 1978
- [2] A. D. Johnson, "Training Phenomena in Nitinol," (IBID, Nitinol Heat Engine Conference)
- [3] A. D. Johnson and S. D. Orlosky, "Electronic Braille Page Output Device Using Nitinol SMA," Phase II Grant Application Dept. of Health and Human Services, Dec. 1986

The research described in this paper was carried out by the Jet Propulsion Laboratory, California Institute of Technology, under a contract with the National Aeronautics and Space Administration.

Reference herein to any specific commercial product, process, or service by trade name, trademark, manufacturer, or otherwise, does not constitute or imply its endorsement by the United States Government or the Jet Propulsion Laboratory, California Institute of Technology.